European Journal of Agronomy 126 (2021) 126278

Contents lists available at ScienceDirect

European Journal of Agronomy

journal homepage: www.elsevier.com/locate/eja

# Field-scale assessment of Belgian winter cover crops biomass based on Sentinel-2 data

Dimitri Goffart [a,*], Yannick Curnel [a], Viviane Planchon [a], Jean-Pierre Goffart [a], Pierre Defourny [b]

[a] Walloon Agricultural Research Centre (CRA-W), Agriculture, territory and technologies integration Unit (U6), Rue de Liroux 9, 5030 Gembloux, Belgium
[b] UCLouvain, Earth and Life Institute/Environmental Sciences (ELI-e), Research Laboratory in Environmetrics and Geomatics, Croix du Sud, 2, 1348 Louvain-la-Neuve, Belgium

ARTICLE INFO

*Keywords:*
Nitrogen recommendation
Catch crops
Remote sensing
Vegetation index
*Sinapis alba*
*Phacelia tanacetifolia*

ABSTRACT

Winter cover crops, used as green manure, can supply up to 45 units of nitrogen per hectare to the following summer crops. In order to contribute to the establishment of the nitrogen balance sheet for fertilisation recommendation of subsequent main crop at field scale, this supply is currently derived from the biomass production, classically estimated visually using 3 classes: 0–1, 1–3, 3+ tons of dry matter per hectare (Mg DM $ha^{-1}$). The capabilities of Sentinel-2 satellite data to retrieve an operator-independent winter cover crop biomass have been assessed. Biomass samples were collected in 1 m quadrats for various types of winter cover fields classically used in Belgium (mustard, phacelia, oat and a range of mixed cover), in 2016 and 2017 (yield between 0.1 to 5 tons of dry matter per hectare). Empirical relationships between the winter cover crop biomass and a wide range of vegetation indices (VIs) derived from Sentinel-2 have been defined, and the most performant VI identified. For pure stands of winter cover crops, the cross-validation RMSE (CVRMSE) of the best model is 0.36 Mg DM $ha^{-1}$ for mustard and 0.3 Mg DM $ha^{-1}$ for phacelia. The CVRMSE observed for mixed stands, around 0.61 Mg DM $ha^{-1}$, is roughly two times higher than the CVRMSE observed for pure stands. The added-value of objective satellite-based estimation of winter cover biomass was also assessed by comparing respective estimations with regards to an independent reference dataset made of sample measurements on the ground. Models based on Earth observation showed better results than farmer visual assessment for mustard crops, and were as good as farmers for phacelia crops.

## 1. Introduction

In intensive cropping systems, nitrogen (N) recommendation methods for main crops have been based for years on the provisional N balance sheet approach, at field scale. The presence of a winter cover crop, used as a green manure/catch crop in the crop rotation, has a significant impact on the N balance. In addition to its positive impact on soil (organic matter, erosion, biological activity, etc.), winter cover crop limits nitrate leaching and makes it available for the subsequent main crop (Besnard and Le Gall, 2000; Justes et al., 2012), supplying, for instance, up to 45 kg N $ha^{-1}$ when considering a mustard crop (*Sinapis alba* sp.) with a biomass production of more than 3 tons of dry matter per hectare (Mg DM $ha^{-1}$) (Cugnon et al., 2013). The level of this effect is linked, in particular, to the winter cover crop type and its biomass production (Destain et al., 2010; Kuo et al., 1996). In order to use specific framework like the Requaferti model, the biomass production is estimated visually through farmers or practitioners according to 3 classes: 0 to 1 (weak), 1 to 3 (medium) and more than 3 (high) tons of dry matter per hectare (Mg DM $ha^{-1}$) (Cugnon et al., 2013).

According to the local technical and extension service structures delivering N recommendation to farmers, collecting such information is not easy and often inaccurate. This situation is exacerbated by the evolution of agriculture in Northwestern European regions: a decreasing number of farmers, an increase in farm size (EUROSTAT, 2018), a loss of farmer historical knowledge regarding the specific field characteristics (due to increasing field renting and cropping operations more and more dedicated to external enterprises). In addition, some observations are just made by visual assessment (e.g. cover crop biomass level), enhancing the variability of the data accuracy.

Facing the resulting operator-dependent nature of the information to

* Corresponding author.
*E-mail addresses:* d.goffart@cra.wallonie.be (D. Goffart), y.curnel@cra.wallonie.be (Y. Curnel), v.planchon@cra.wallonie.be (V. Planchon), j.goffart@cra.wallonie.be (J.-P. Goffart), pierre.defourny@uclouvain.be (P. Defourny).

https://doi.org/10.1016/j.eja.2021.126278
Received 15 June 2020; Received in revised form 8 March 2021; Accepted 10 March 2021
Available online 4 April 2021

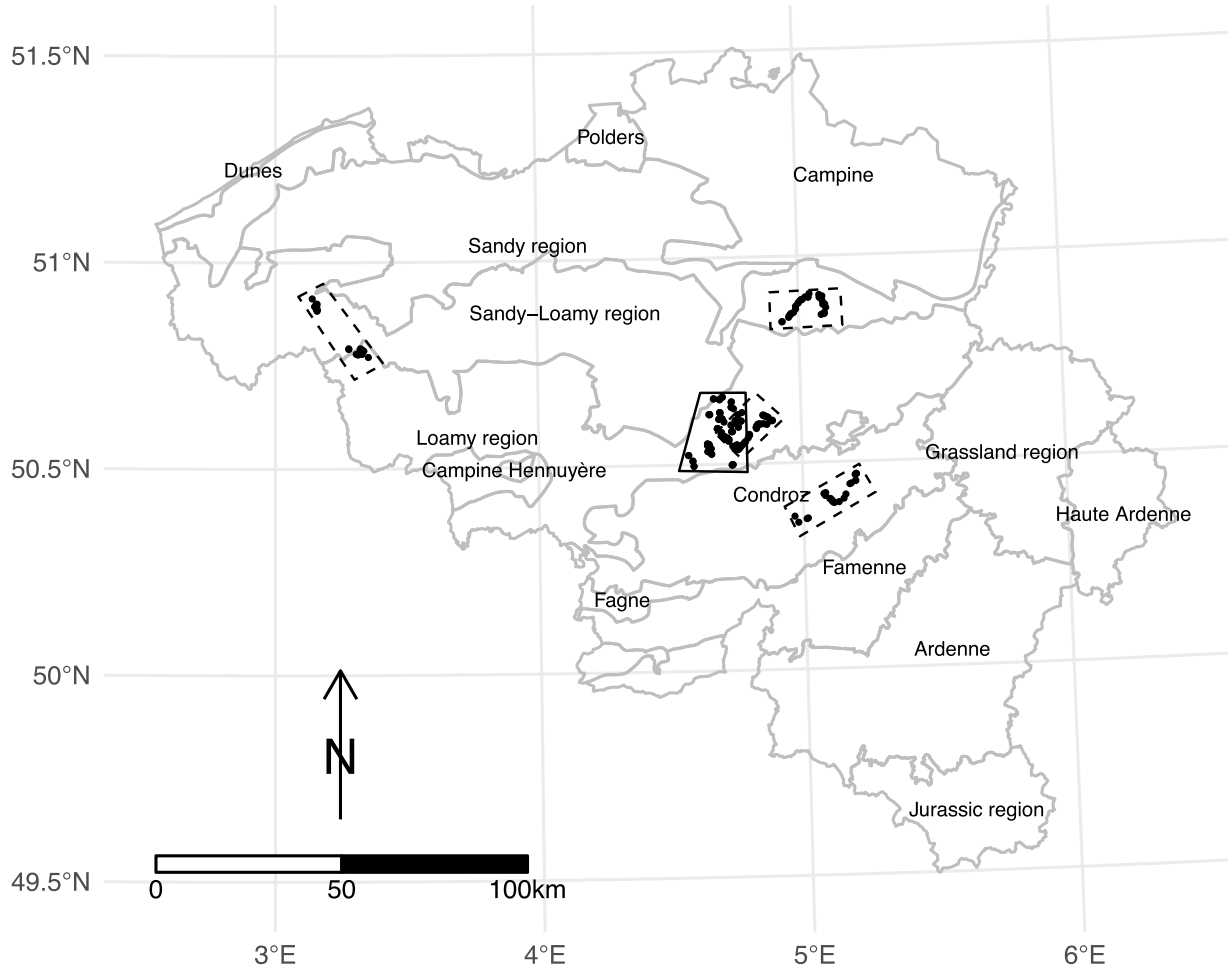


**Fig. 1.** Location of the areas of interest (AOI) for winter cover crop species identification and biomass sampling campaign in 2016 and 2017 (continuous line) and for winter crop species identification and plant height measurement in 2017 (dashed line). The Belgian agricultural regions containing these AOI are mentioned. (Projected coordinate reference system: WGS 84/UTM zone 31N).

be collected, there is a real need to develop new global tools to support the collection of accurate and operator-independent information, aiming to contribute to relevant N recommendations. The recent launch of new European satellites such as Sentinel-2a/2b (S2), largely designed for agriculture monitoring at field scale, open new opportunities to reach such an objective (ESA, 2012). Their spatial, temporal, spectral and radiometric resolutions, together with their systematic acquisition strategy and free-access policy, are expected to supply enhanced Earth observation products (Jaramaz et al., 2013) triggering the development of a new approach for N-recommendation.

Vegetation indices (VIs) are widely used for the estimation of vegetation biomass or other biophysical variables (BVs) such as leaf area index (LAI) (Kalaitzidis et al., 2009; Xue and Su, 2017). Vina et al. (2011) demonstrate the possibility to estimate maize and soybean LAI using one unique VI derived from close range and aircraft mounted sensor images, despite their contrasting vegetation structure. Frampton et al. (2013) assessed the capacity of S2 to retrieve crops LAI, leaf chlorophyll concentration and canopy chlorophyll content (CCC), through their relationship with several VIs. Clevers et al. (2017) showed that potato LAI and CCC can be estimated accurately with S2 10 m bands only, while Delegido et al. (2011) proved the importance of the 20 m S2 red-edge (RE) bands for the estimation of LAI and CCC of numerous crop types.

More specifically, several studies have shown the potential for remote sensing (RS) to retrieve winter cover crop biomass, through the relationship between VIs and the biomass, using a proximal sensor such as cropscan (Prabhakara et al., 2015), sensor mounted on unmanned aerial vehicle (Hunt et al., 2013; Yuan et al., 2019) or SPOT-5 satellite sensor (Hively et al., 2009). These studies considered exclusively graminaceous winter cover crop like wheat, barley, rye or ryegrass, used as main crops after the winter season, and, except for Prabhakara et al. (2015) who also used a RE band, the VIs calculated are limited to the use of green, red, and near infrared (NIR), showing good results until 1 to 2 Mg DM $ha^{-1}$ and saturation issues for higher biomass.

This paper aims at assessing the capabilities of S2 data to retrieve 'Belgian' winter cover crop biomass production. The cover crops considered can reach biomass up to 5 Mg DM $ha^{-1}$ and are pure stand mustard (*Sinapis alba* sp.), phacelia (*Phacelia tanacetifolia* sp.) and oat (*Avena sativa* L.) crops, and different types of mixed cover crops (two to four different species). Empirical relationships between the winter cover crop biomass and 73 VIs have been established from the blue, green, red, three RE, two NIR and two short-wave infrared (SWIR) bands. In order to quantify the RS added-value with regards to visual farmer-based estimation, biomass estimation obtained from satellite RS data and from visual assessment have both been compared with reference field measurements.

## 2. Material and methods

### 2.1. Location and types of collected data

The field data collected in this study concerned winter cover crop

species identification, biomass sampling and plant height measurement. In 2016 and 2017, species identification and biomass samples were collected along with height measurement (only in 2017), in the vicinity of Gembloux (loamy soils; continuous line area in Fig. 1). In 2017, winter cover crop species identification and plant height measurements were collected in four additional areas, distributed in contrasting Belgian agricultural regions differing for pedo-climatic conditions (dashed line area in Fig. 1) and including sandy-loamy, loamy and stony-loamy soils. The choice of these additional areas in 2017 was linked to two factors: the importance of the area covered by winter cover crops within the different Belgian agricultural regions and related legislative management restrictions (*i.e.* authorized winter cover crop burial date that can differ between regions, (SPW, 2017)).

### 2.2. Field data sampling procedures

#### 2.2.1. Biomass sampling

The first biomass sampling campaign was organised in November 2016. This campaign only focused on white mustard (*Sinapis alba* sp.), widely used as a winter cover crop in Belgium. Twenty-three fields presenting visually differing levels of aerial biomass had been selected. Four aerial biomass samples (geolocalized with a hand-held GPS device) had been collected per field in 1 sqm quadrats on the 8th and 10th of November 2016. Each sampling point was located at least 50 m from the field border and in a homogeneous biomass zone (visually assessed). The flowering percentage was visually assessed and classified (0–25, 25–50, 50–75, 75–100% of the plants in bloom). Collected biomass samples were directly sealed in plastic bags, to avoid water losses, and then fresh weighed in the laboratory. A representative subsample of about 500 g was oven-dried at constant temperature (80 °C) for a minimum of 72 h up to constant weight, to determine the dry matter content (%), and to derive the dry matter biomass (DMB) production (Mg DM $ha^{-1}$).

A second campaign was organised in October 2017 using the same protocol. The biomass sampling also concerned white mustard, and was extended to three additional winter cover crop types: phacelia (*Phacelia tanacetifolia* sp.), oat (*Avena sativa* L.) and mixed cover crops. Mixed cover fields correspond, most of the time, to ecological focus areas as defined by the Common Agricultural Policy (SPW, 2017). These are composed of two to four different species, which are mainly phacelia, mustard, oat and fodder radish, or also vetch, sunflower, clover, field bean and pea. Forty-two fields were sampled from the 15th to the 31th of October 2017. The number of samples per field ranged from 4 to 8. In total, 180 biomass samples were collected. The number of samples for white mustard, phacelia, oat and mixed cover was respectively equal to 36, 42, 20 and 82. The botanical composition of each mixed cover was recorded.

#### 2.2.2. Biomass proxy

The vegetation height can be used as a biomass proxy. It was measured during the 2017 campaign at each of the 180 biomass sampling points, and also in 136 other winter cover crop fields (7, 10,14 & 22nd of November 2017), in the four areas of interest (AOIs) described in Fig. 1. In these 136 winter cover crop fields, the height was measured four times next to a geolocated point, located at least at 50 m from the field boundary.

#### 2.2.3. Visual estimation of biomass classes

The farmer-based estimation of biomass for provisional N balance sheet method is in essence subjective and qualitative: 0 to 1 (weak), 1 to 3 (medium) and more than 3 (high) Mg DM $ha^{-1}$. It is also subject to uncertainties, due to the time lag between the cover crop ploughing, generally operated in November/December, and farmer estimation usually 2 to 4 months later, when the provisional N balance sheet is established. To assess the added value of RS data, expected to be more objective and accurate, the farmers visual estimation of these classes was collected between the end of February and mid April 2017 and 2018 for most of the fields sampled in autumn 2016 and 2017 respectively.

**Table 1**
Sentinel 2 optical images selection for years 2016 and 2017.

| Year | Operational S2 | Selected dates |
|---|---|---|
| 2016 | S2A | 08–16, 08–26, 09–08, 09–25, 10–08, 10–15, 12–04 |
| 2017 | S2A &S2B | 08–29, 09–25, 10–15, 10–18, 10–30, 11–07, 11–17, 11–22 |

### 2.3. Meteorological data

Daily meteorological data from the Ernage weather station, belonging to the Belgian Royal Meteorological Institute, located in the sampling AOI, were retrieved for September, October and November 2016 and 2017. The minimum temperature at 1.5 m, and grass minimum temperature at 10 cm height, were used to assess the winter cover crops growing conditions.

### 2.4. Satellite data

Five 2016 and eight 2017 S2 optical images with few or no clouds (less than 20% in the sampling AOI) were selected over the winter cover crops growing periods, *i.e.* between mid-August and the end of November (Table 1). Images were atmospherically corrected using the OPERA algorithm processing (Sterckx et al., 2015). The 10 and 20 m resolution reflectances of the S2 multi spectral instrument were used for calculation of the VIs list in appendix A. This selection results from a thorough literature review and regroups VIs related to crop biomass or crop biomass proxies with a view to assess multiple possible combinations of bands allowed by S2. In particular, as suggested by Jaramaz et al. (2013) and Delegido et al. (2011), the use of the RE bands should enhance the estimation of crop biophysical parameters, like LAI, which is directly related to aerial biomass. Three BVs were also considered: the fraction of photosynthetically active radiation (*f*APAR), the fraction of vegetation cover (*f*COVER) and LAI, retrieved through the inversion of the BV-NET radiative transfer model using height bands of S2: green (B03), red (B04), RE (B05, B06, B07), NIR (B8A) and SWIR (B11, B12), as described by Weiss and Baret (2016).

### 2.5. Methods

The methodology developed in this study, aiming to estimate winter cover crops biomass (classes) based on S2 data has been motivated, as aforementioned, by a supposed misestimation of this information by farmers. In order to check this assumption, field-based estimates of winter cover DM biomass classes were first compared to the *a posteriori* estimates provided by farmers. This assumption being validated, the next step aimed at the identification of the best combinations of VIs and statistical models for estimating winter cover biomass using a cross-validation approach. The selected relationships were afterwards also validated on an independent data set (biomass proxy). The added value of using satellite data was finally assessed based on a comparison with farmers visual assessment. Because of satellite images availability issues in 2016 (detailed in the results section), 2016 data were only used in the first step of the methodology.

#### 2.5.1. Fields and farmers data comparison

Sampled DMB data were averaged by field and categorised in the three classical classes described above, in order to compare it with the farmer's assessment through a confusion matrix.

#### 2.5.2. Data extraction and VIs calculation

Using samples GPS positions, 10 and 20 m S2 reflectances, as well as BVs, shadow mask and cloud mask were extracted from the selected images using a buffer of 20 m radius around the sampling point,

**Table 2**
Models tested for the relation between the vegetation index value ($x$) and the dry matter biomass per hectare ($y$).

| Model | Transformed variable for linearisation | Formula |
|---|---|---|
| Linear regression | / | $y = a + b \,.\, x$ |
| Order 2 polynomial regression | / | $y = a + b \,.\, x + c \,.\, x$ |
| Linear regression | $x$ | $y = a + b \,.\, exp(x)$ |
| Linear regression | $x$ | $y = a + b \,.\, x$ |
| Exponential model | $y$ | $y = a \,.\, e^{bx} \Leftrightarrow ln(y) = ln(a) + b \,.\, x$ |
| Power model | $y$ and $x$ | $y = a \,.\, x^{b} \Leftrightarrow ln(y) = ln(a) + b \,.\, ln(x)$ |

resulting in a mean value for each sample from 12 to 14 pixels at 10 m resolution and 2 to 4 pixels at 20 m resolution. Data was filtered using the cloud and shadow masks. S2 images were checked at the sampling points positions to apply a manual correction of these masks, and ensure any later issues linked to misclassified masks pixels. VIs (Table A.4) were then computed. Considering the non-systematic coincidence between the sampling and the S2 acquisition dates and a time lag of 5 days maximum, VIs and BVs values have been estimated for each sampling date, based on linear regressions between the two surrounding dates.

### 2.5.3. Assessment of the relationships between VI/BV values and DMB

A visual assessment of the VI – DMB relationships tend to show a saturation of VI/BV values at high biomass. Several models and variables transformation have been considered for assessing the relationship between VI/BV and DMB (Table 2). For each relationship, the coefficient of determination ($R^2$) and the root mean square error (RMSE) were retrieved. In order to better evaluate the strength of the relationships between the remotely-sensed VI/BV and the field data, a 10-fold cross-validation has been used and the cross-validation RMSE (CVRMSE) computed. This was applied to the whole dataset (mixed, phacelia, mustard and oat) and separately on the four cover crop types. The possible effect of flowering on the defined relationships was investigated. The models with the lower CVRMSE were selected, and the time series of the VIs/BVs used in these models, visually assessed.

As a saturation in the selected VIs/BVs was still noticed, the two VIs approach developed by Nguy-Robertson et al. (2012) for LAI estimation issues, was tested to mitigate this limitation. Data set was divided into two groups based on observed biomass: lower and higher than 2 Mg DM ha$^{-1}$. The choice of this DMB value to separate the two groups was based on a visual assessment of the first approach VI/BV – DMB relationships saturation. The same methodology as described above was applied to both groups separately. In the results, the first approach (one VI) and the second approach (two VIs) are called respectively approach 1 and approach 2.

### 2.5.4. Model validation with biomass proxy

Relationships between DMB and crop height have been established per crop type based on 2017 field data. The quality of each model was assessed by a 10-fold CVRMSE. These models were used to estimate the DMB for the 136 fields where only height measurements were taken in 2017. These estimated DMB were used as validation data sets. S2 data were extracted and interpolated (at the height measurement dates) in the same way as already described above (but only with one geolocated point per field). For each cover crop type, the best VI value-DMB model selected was applied to predict the response value and then the validation RMSE was calculated.

### 2.5.5. RS data added value assessment

Farmers providing an estimation of biomass classes at field level, reflectance data extracted at this level and the VIs corresponding to the best models previously identified, have been computed for the selection of satellite images available for mid-October to mid-November and filtered using the cloud/shadow masks (at the field level). For each field, reduced with an inner buffer of 15 meters to avoid border effects and shadows, these models have been applied considering the maximum VI value reached over this period in order to get the DMB value and its class considered in the provisional N balance sheet. The choice of considering the maximum VI values has been guided by the fact that the biomass estimation provided by farmers corresponds to the maximal observed situation, and by the *a priori* positive relationships of the considered models. The biomass classes estimated by farmers and those based on satellite data have been compared to the observed biomass classes through an error matrix. The comparison of the true positive rates, and accuracy, allowed an assessment of the added value of remotely-sensed estimation of biomass class compared to the estimation provided by farmers.

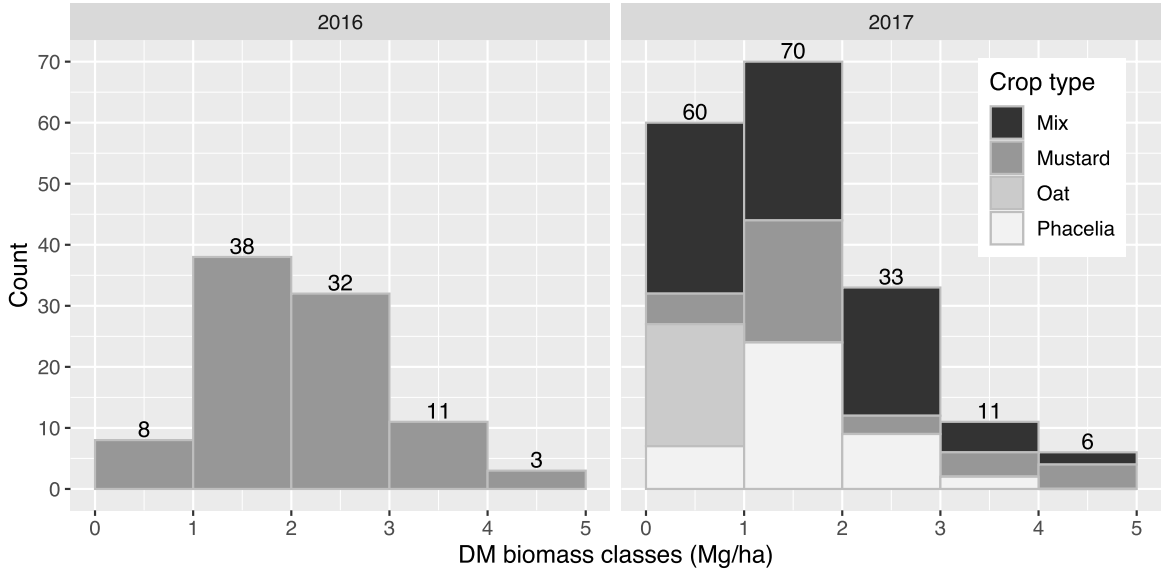


**Fig. 2.** Distribution of sampled dry matter biomass per winter cover crop type and per year.

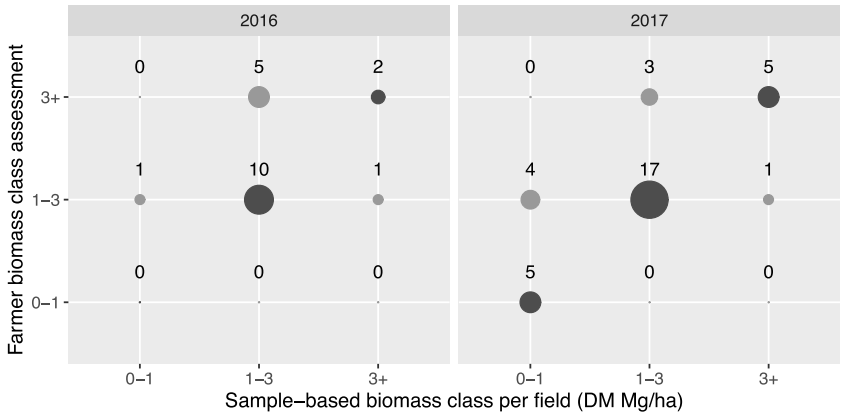


**Fig. 3.** 2016 and 2017 error matrix of the farmers biomass class assessment (whole field) with sample-based biomass class as reference value (samples average).

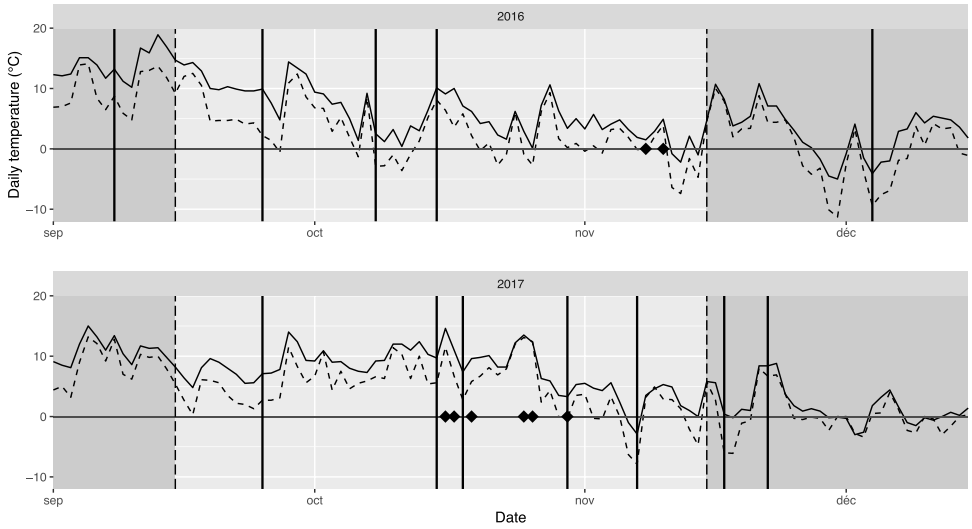


**Fig. 4.** 2016 and 2017 timelines of used Sentinel-2 images (vertical lines), biomass sampling dates (diamond) and evolution of the minimum temperature in the sampling area of Gembloux (black line = minimum temperature under shelter at 1.5 m, dash line = minimum temperature at 10 cm on grass). Vertical dash lines for each figure = Legal dates for end of sowing and start of destruction of winter cover crop in Wallonia.

## 3. Results

### 3.1. Winter cover crop biomass assessment

#### 3.1.1. Distribution of the samples

Distribution of sampled biomasses per crop type is presented in Fig. 2 for both years. Although all the 3 biomass classes considered in the provisional N balance sheet are represented, most of the samples belong to the intermediary class (1-3 Mg DM $ha^{-1}$) whatever the winter cover crop type and the year. An exception can be, however, observed for pure stands of oats represented by a limited number of samples all belonging to the lowest biomass class (< 1 Mg DM $ha^{-1}$). For this reason, this winter cover crop type was not considered separately in our analysis but is still included in what is called later the full category, including the whole dataset.

#### 3.1.2. DMB estimation by farmers

As far as samples are considered as representing the monitored fields, comparisons of sampled and farmers-estimated biomass classes (Fig. 3) show an obvious overestimation of biomass classes by farmers. The overall accuracy is equal to 63% (12 fields correctly classified over 19) and 77% (27 fields correctly classified over 35) respectively for 2016 and 2017. True positive rates are, respectively for the three classes, in 2016, 0, 53, 11%, and in 2017 14, 49, 14%. These classification errors justify the objectives followed in this paper.

#### 3.1.3. Satellite data availability and meteorological conditions

Fig. 4 presents the time series of the satellite images used in this study, the air temperatures at 1.5 m and grass minimum temperature at 10 cm for both years. A low availability of usable images can be clearly observed for 2016. This low availability is linked to the frequent cloudy conditions met during this period, and the fact that Sentinel-2B, launched in March 2017, was not yet available. No valid images were available between the 15th of October and the 4th of December 2016. Considering that samples were collected on the 8th and 10 November 2016, the number of days between image acquisition and sampling dates is important, varying between 24 and 28 days.

Walloon legislation authorises the destruction of winter cover crops from the 15th of November (SPW, 2017). S2 images acquired on the 4th of December 2016 allowed assessment that only 6 of the 23 fields had not yet been destroyed (the other 17 parcels presenting reflectances characteristic of bare soil). According to Labreuche (2009), the temperature at 2 m height inducing critical freezing damage is between −5 and −10 °C for mustard. Fig. 4 can show that this threshold was reached, after the sampling dates, at the end of November. It can therefore be assumed that the vegetation in the 6 remaining parcels has been clearly impacted by frost. Estimating a VI value at sampling dates based on usable S2 images, acquired before and after these dates, is therefore not

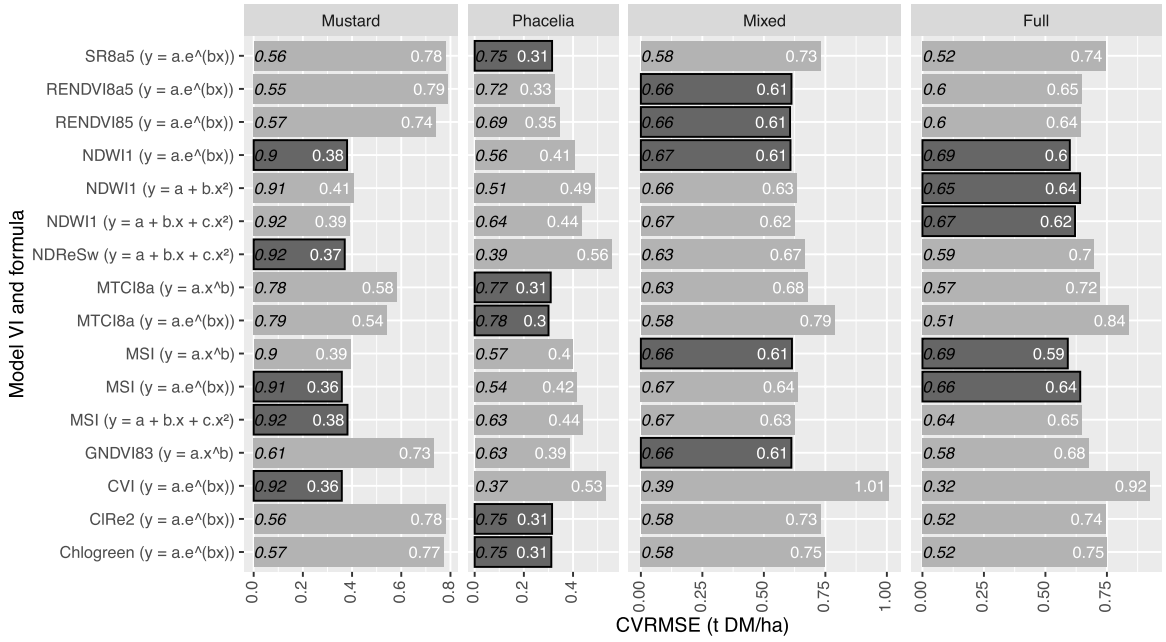


**Fig. 5.** Based on 10 fold cross-validation RMSE, top 5 of the models tested (highlighted bars) for the 2017 whole dataset (full), for mixed cover, for mustard and for phacelia. The italic black number is the $R^2$ of the model.

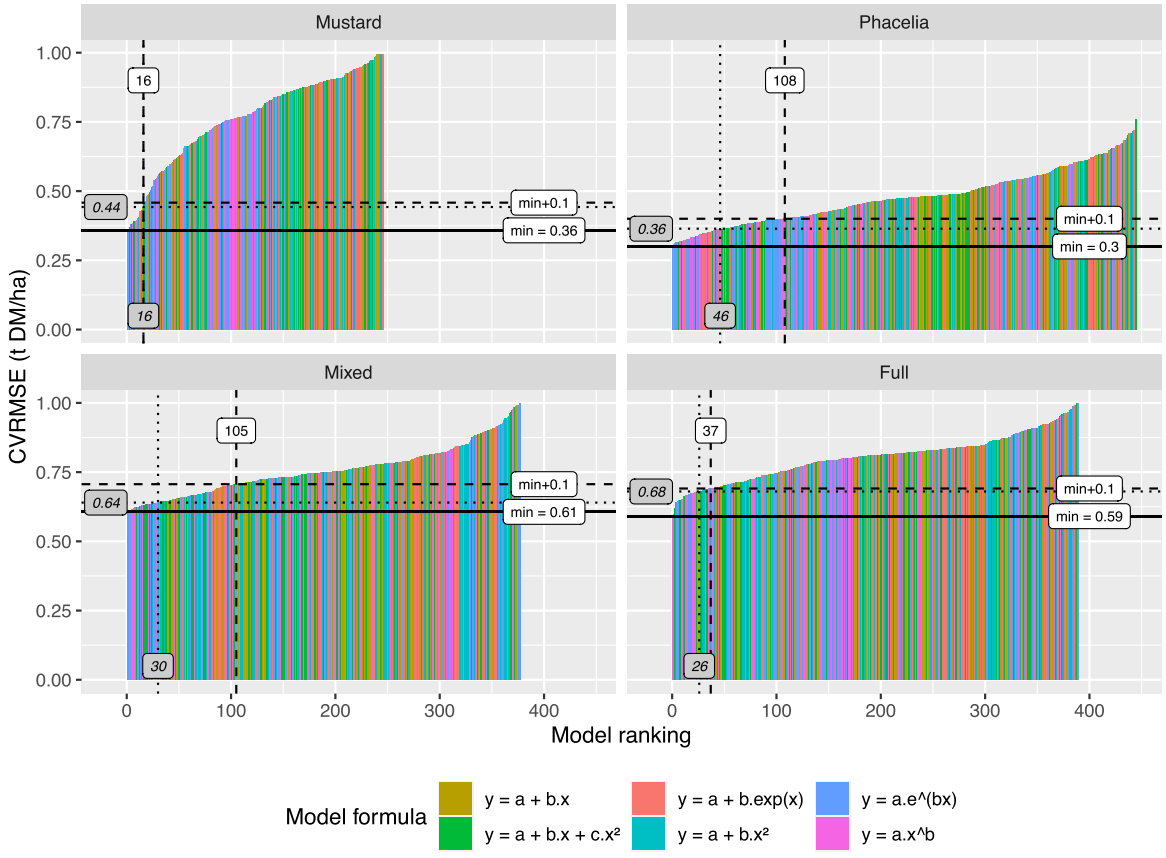


**Fig. 6.** Models ranking by cross-validation RMSE (CVRMSE) for each category (only situations with a CVRMSE lower than 1 are presented) on 2017 data. Total number of models tested per category is 456 (combination of 76 VIs/BVs with 6 different model types). The solid lines represent the minimum observed CVRMSE values, the dashed lines this minimum value + 0.1 Mg DM ha$^{-1}$ and the ranking position of the model just under this threshold, the dotted lines the CVRMSE for the bests simple linear regressions and the corresponding ranking position. Note that for Mustard, the vertical dotted and dashed lines are at the same ranking position.

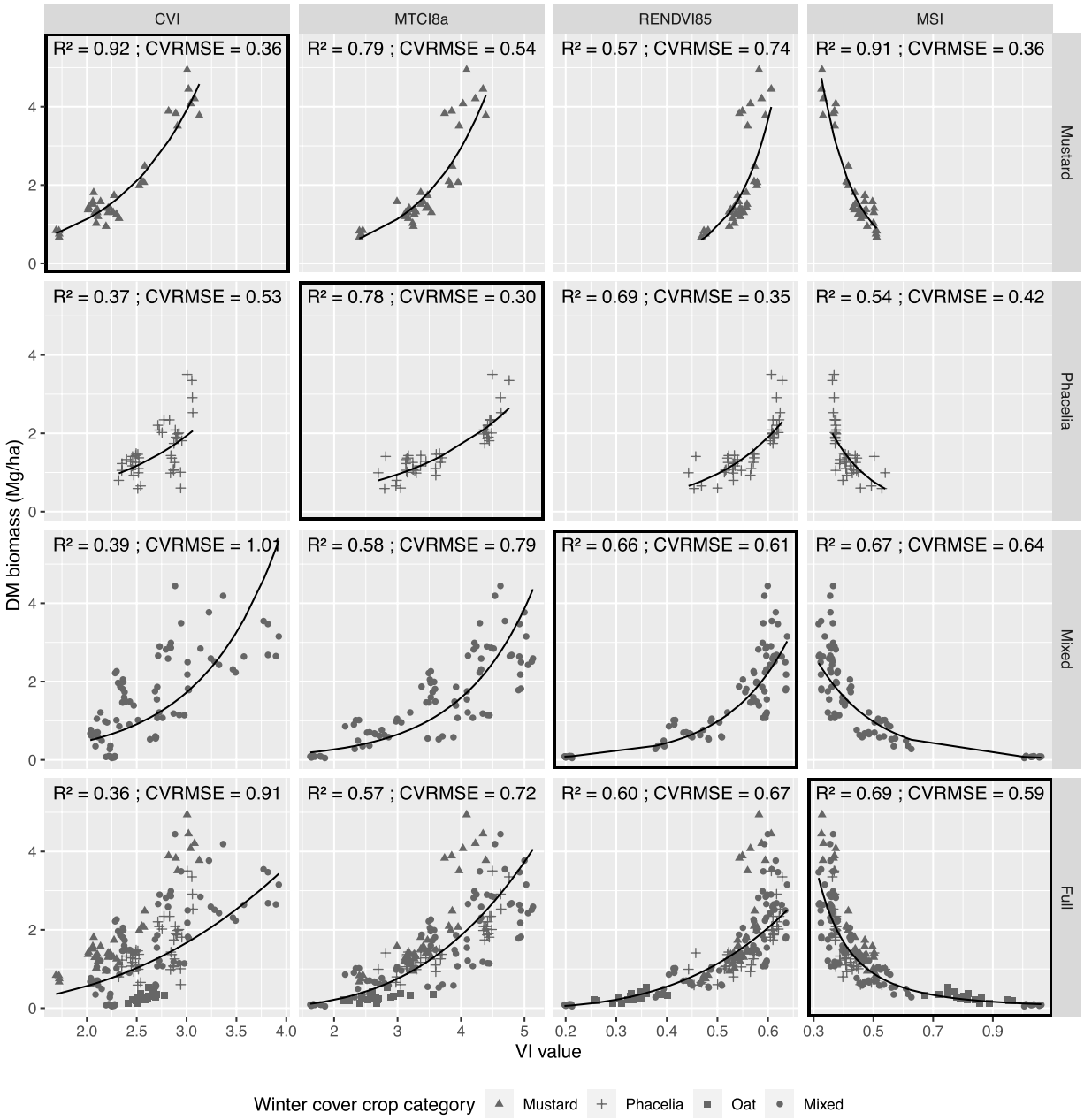


**Fig. 7.** Best VI-DM biomass model by category (highlighted diagonal of graphs) on 2017 data. CVI, MTCI8a and RENDVI85 used with an exponential model. MSI used with a power model.

possible in 2016.

In 2017, the occurrence of usable images is higher, and allows estimation of VI value at sampling date. The time lag between the sampling and the satellite acquisitions is a maximum of 5 days. The relationships between DMB and VI values is therefore only assessed for 2017 data.

### *3.1.4. Identification of the best models (approach 1) per winter cover category*

In this study, a model should be understood as a combination of a model type (e.g. linear regression) and a VI (e.g. MTCI). In total, more than 450 models were tested (6 model types × 76 VIs/BVs). The selection of the five best models per winter cover crop category, based on the 10-fold CVRMSE, is presented in Fig. 5. Best models usually consider an exponential ($y = ae^{bx}$) or a power ($y = ax^b$) relationship (Figs. 5 and 6). For pure stands, the CVRMSE of these 5 best models varies between 0.36 and 0.38 Mg DM ha$^{-1}$ for mustard, and between 0.3 and 0.31 Mg DM ha$^{-1}$ for phacelia. $R^2$ is around 0.9 for mustard and 0.75 for phacelia. According to CVRMSE, phacelia models perform better than mustard models while it is the contrary according to $R^2$. This is explained by the high difference of DMB average, influencing the calculation of $R^2$: 1.99 Mg DM ha$^{-1}$ for mustard and 1.57 Mg DM ha$^{-1}$ for phacelia. The CVRMSE observed for mixed category and full category, around 0.6 Mg DM ha$^{-1}$, is roughly two times higher than the CVRMSE observed for pure stands. $R^2$ is around 0.67 for both categories. Average DMB value is 1.60 Mg DM ha$^{-1}$ for mixed stands and 1.53 Mg DM ha$^{-1}$ for full category. This is comparable to the phacelia category DMB average.

Fig. 6 shows that the difference of CVRMSE between models is sometimes limited. For instance, in the full category, the best model presents a CVRMSE of 0.59 but 37 models presenting a CVRMSE lower than 0.69 Mg DM ha$^{-1}$ (0.59+0.10) can be identified representing 8.1% of the models tested. For mixed category, 23% of models have a

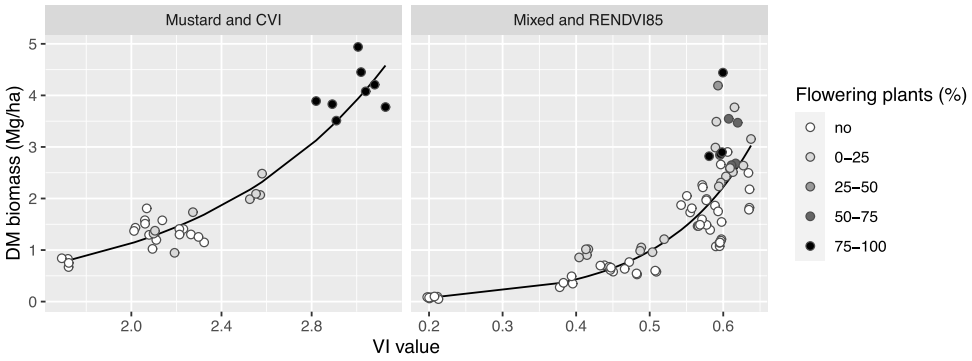


**Fig. 8.** Best VI-DM biomass model with flowering percentage indications for mustard and mixed categories on 2017 data (no flowering was observed in the sampled *Phacelia* fields).

CVRMSE of less than 0.7 Mg DM ha$^{-1}$ (the CVRMSE of the best model being equal to 0.6). For mustard, 3.5% of the models have a CVRMSE lower than 0.46 Mg DM ha$^{-1}$ and for phacelia, 23.7% less than 0.4 Mg DM ha$^{-1}$. This figure shows also that the linearisation methodology is useful particularly for mustard and full categories where the difference between the best model and the best simple linear model reaches nearby 0.1 Mg DM ha$^{-1}$. This difference is less pronounced for phacelia (0.06) and even less for mixed category (0.03). For this last category, a simple linear regression could be used instead of the exponential model.

Within each category, the top five (Fig. 5) highlights two (for full) to five (for mixed) VIs that are strongly correlated. Except for the NDReSw, all indices use the B8 or B8A bands (NIR) in combination with one or two other bands. The other bands used are B03 (green), B04 (red), B05 (RE), B06 (RE), B11 (SWIR), B12 (SWIR). The MSI and the NDWI1 are in the top 5 for three of the four categories. Both of them are calculated with a combination of B8A and B11 S2 bands.

### 3.1.5. *Best model by category (approach 1)*

The best model for mustard, phacelia and mixed cover use respectively the Chlorophyll Vegetation Index (CVI, from Vincini et al., 2008 *In:* Clevers et al., 2017), the MERIS Terrestrial Chlorophyll Index (MTCI8a, using B8A instead of B6, from Dash and Curran, 2004 *In:* Vina et al., 2011) and one of the multiple possibilities of Red-Edge Normalized Difference Vegetation Index (RENDVI85, suggested by Delegido et al., 2011) with an exponential model and have respectively a CVRMSE of 0.36, 0.30 and 0.61 Mg DM ha$^{-1}$ (Fig. 7). The corresponding linear relationships, which involve a transformation on $y$, have a $R^2$

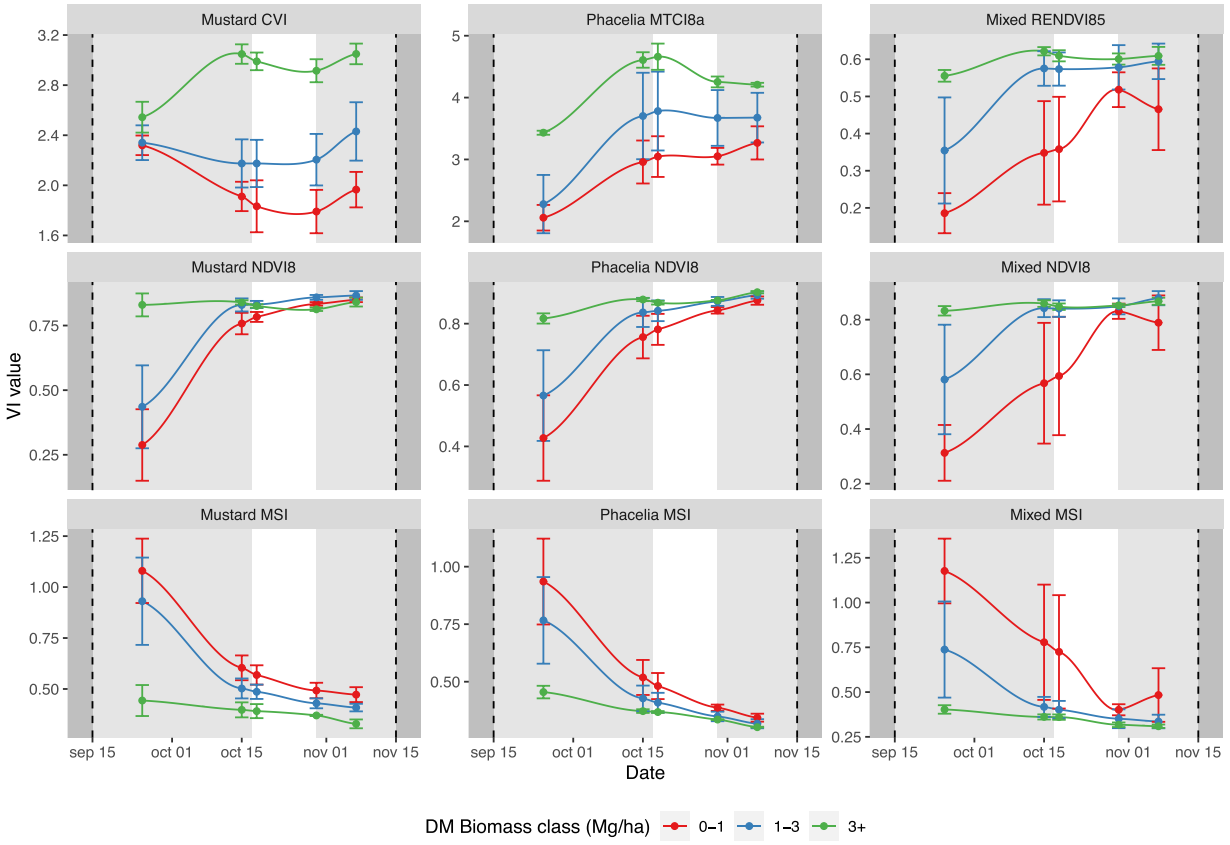


**Fig. 9.** DM biomass classes mean VI value time series, for each winter cover crop type (2017 data). The VIs are the four best VIs selected for each of the four cover crop types (mustard: CVI, phacelia: MTCI8a, mixed: RENDVI85, full: MSI). The NDVI is added to allow a comparison with this widely used VI. Error bar = standard deviation. White area = sampling period. Dashed lines = Legal dates for end of sowing and start of destruction for winter cover crops in Wallonia.

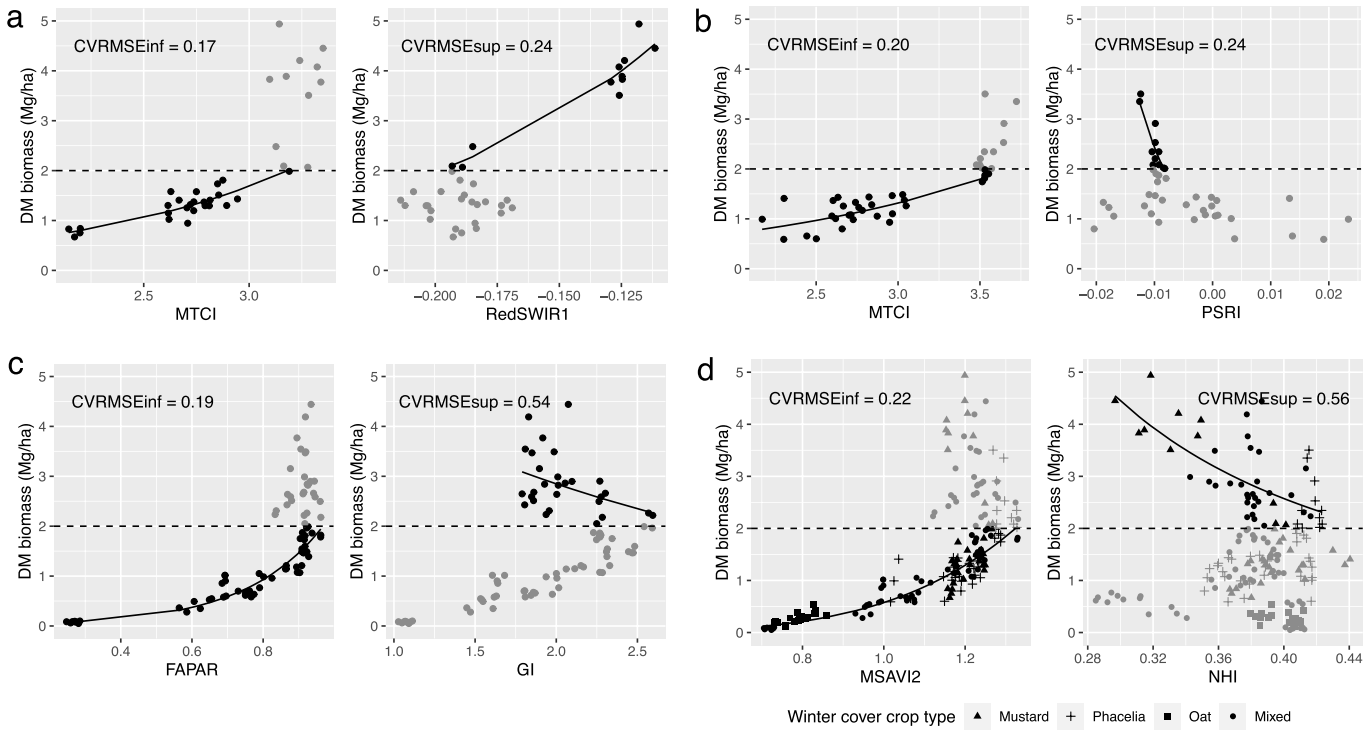


**Fig. 10.** Best VI-DMB models by category (according to the 10 folds cross-validation RMSE), considering the separation of biomass in two classes (inferior to 2 Mg DM ha$^{-1}$ to the left, and superior to 2 Mg DM ha$^{-1}$ in the middle) resulting in the use of two different indices and relationships by category winter cover crop (approach 2). Exponential model for mustard (a), phacelia (b) and mixed (c), using respectively MTCI & RedSWIR1, MTCI & PSRI, FAPAR & GI. Power model for full category (d), using MSAVI2 & NHI.

respectively equal to 0.92, 0.78 and 0.66. Among these three VIs, CVI is the more specific to one category according to the low $R^2$ when it is used for another category than mustard. MTCI8a is less specific and RENDVI85 even less. For the full category, the best model is a power model based on the Moisture Stress Index (MSI, from Rock et al., 1985 *In:* Radoux et al., 2016). This model presents a CVRMSE of 0.59 Mg DM ha$^{-1}$ and the linear relationship, which involves both a transformation on $x$ and $y$, has a $R^2$ of 0.69. Contrary to the three previous VIs mentioned, MSI shows a negative correlation with the DMB. When applied on the other category, MSI is as good as CVI for mustard, and performant for mixed category, while it shows bad results for Phacelia compared to MTCI8a of even RENDVI85.

Several studies have highlighted the influence of flowering on reflectances, and subsequently on VIs (Fang et al., 2016; Sulik and Long, 2015). For mustard (Fig. 8), a relationship between the vegetation indice (CVI) values and the flowering percentage seems to be observed; higher CVI values corresponding to higher flowering percentage, but also to higher biomass. This trend is less significant for mixed covers. Flowering is mainly regulated by environmental factors, such as photoperiod or vernalization, but can also be induced by stress factors such as nitrogen deficiency (Takeno, 2016). A relationship between biomass and flowering is therefore theoretically not straightforward. Our available data set (especially the lack of data with a high flowering percentage and low biomass) does not unfortunately allow us to determine the possible effect of biomass and flowering on reflectances.

As depicted in Fig. 9, the CVI allow a good discrimination of biomass classes during the sampling period, while for the other three indices a saturation seems to be observed making discrimination of high classes more difficult (especially for MSI). These indices seem, however, to allow a better discrimination of classes earlier in the growing season. The first value in the CVI time series seems aberrant for the first two biomass classes. At this time, the ground is most probably bare or almost

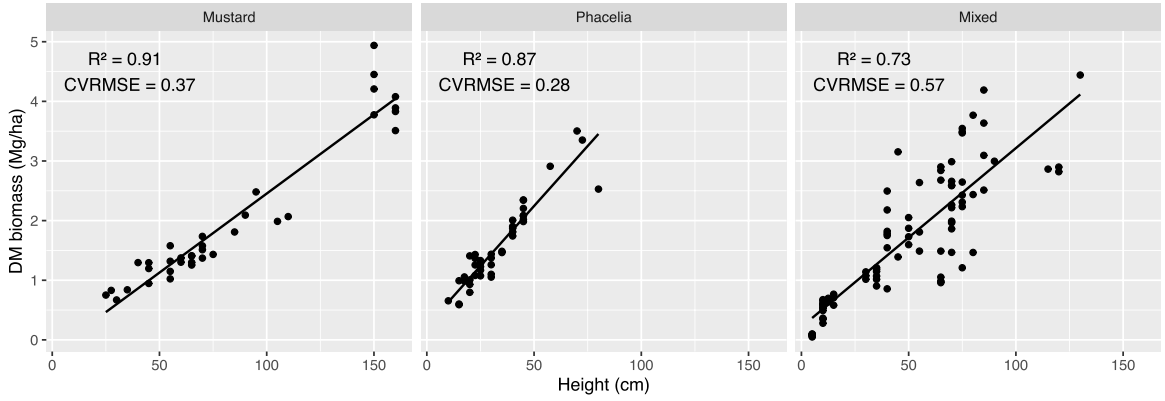


**Fig. 11.** Relationship between the vegetation height and the dry matter biomass for different winter cover crop types (2017 data). CVRMSE = mean RMSE from 10 folds cross-validation.

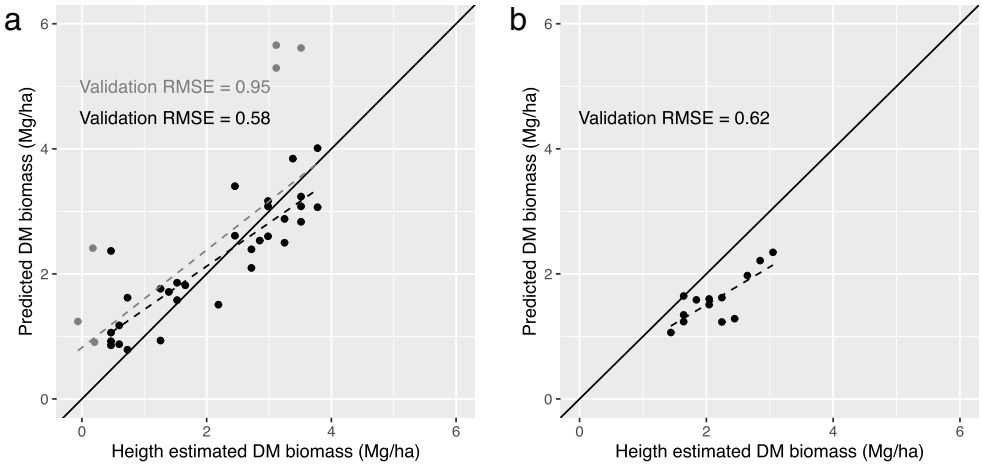


**Fig. 12.** Validation of the mustard (a) and phacelia (b) VI-DM biomass models using truth biomass estimated by height measurement. Black line = identity line ($y = x$). For mustard, two 10 folds cross-validation RMSE values are displayed: one for the whole dataset available (grey), the other excluding the data out of models range values (three low biomass values linked to a lower height than height-DM biomass model min value and three high biomass values linked to a higher CVI than the VI-DM biomass model max value).

bare, which is confirmed by the NDVI time series observation. The CVI seems to be impacted by bare soil and a sufficient cover of the ground is necessary to obtain a reliable biomass estimation.

The error bar shows the standard deviation. Globally, it is higher for low biomass classes and lower for high biomass classes. This can be linked to the saturation but not exclusively. For the mixed category, the very high standard deviation value for the lowest biomass class is linked to the distribution of a group of biomass samples that include biomass near 0 Mg DM ha$^{-1}$ (Fig. 7), which present reflectance close to a bare soil, inducing a high variability inside the 0-1 Mg DM ha$^{-1}$ class.

### 3.1.6. Exploring the possibility to use two VIs (approach 2)

Fig. 10 presents the best models identified for each considered winter cover crop category when relationships between observed biomasses and VIs are defined considering separately 2 groups of biomass (lower and higher than 2 Mg DM ha$^{-1}$). CVRMSE for this second approach can be considered as the average value between CVRMSEinf and CVRMSEsup. This approach allows us to reach significantly lower CVRMSE than the previous one. It decreases from 0.36 to 0.21 Mg DM ha$^{-1}$ for mustard, from 0.30 to 0.22 Mg DM ha$^{-1}$ for phacelia, from 0.61 to 0.37 Mg DM ha$^{-1}$ for mixed cover and from 0.59 to 0.38 Mg DM ha$^{-1}$ for full category. CVRMSEinf is quite similar between the four categories, suggesting that it would be performant to use a unique relation for all crop types for biomasses under 2 Mg DM ha$^{-1}$. CVRMSEsup results show that higher biomass values remain not well estimated for mixed and full categories. The high biomass are negatively correlated with the selected VI for phacelia, mixed and full categories.

## 3.2. Validation using biomass proxy data

The relationship between the vegetation height and the DMB for the different winter crop types is presented in Fig. 11. The $R^2$ (the CVRMSE) is equal to 0.91 (0.39 Mg DM ha$^{-1}$), 0.87 (0.28 Mg DM ha$^{-1}$) and 0.72 (0.59 Mg DM ha$^{-1}$) respectively, for mustard, phacelia and mixed winter cover. Considering the weakest relationship observed for mixed winter cover crops, the validation based on biomass has not been performed for this crop type.

Results of this validation for mustard and phacelia are presented in Fig. 12. Some data were out of the range of the models for mustard (grey points on the figure). Three low biomass values were linked to a lower height than the height-DMB model min height value and three high biomass values were linked to a higher CVI value than the VI-DMB model max CVI value. The validation RMSE decreases from 0.95 to 0.58 Mg DM ha$^{-1}$ when putting these 6 values apart. Considering the

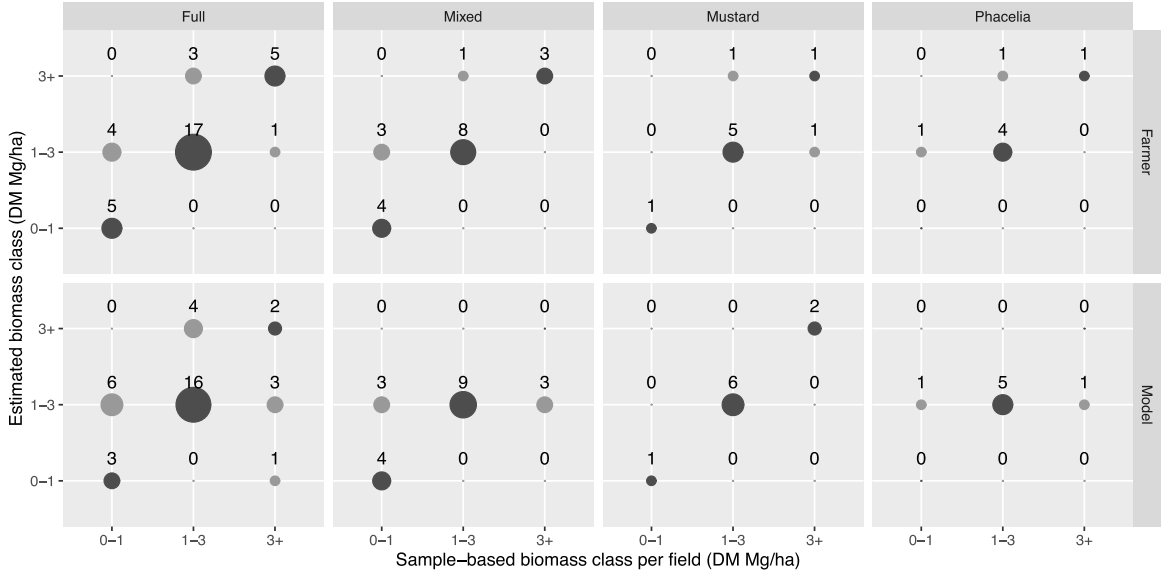


**Fig. 13.** Error matrix of winter cover crop types biomass values at field level distributed over different classes, assessed from farmer-based or RS models-based approaches and compared to the distribution over similar classes of sample-based biomass values considered as a reference (2017 data).

**Table 3**
Overall accuracy of farmers-based and RS models-based biomass class estimations compared to the reference sample-based biomass at field level (detailed classifications in Fig. 13), for different types of winter cover crop (2017 data).

| Category | Parcels | Farmer accuracy (%) | Model accuracy (%) |
|---|---|---|---|
| Full | 35 | 77 | 61 |
| Mixed | 14 | 79 | 68 |
| Mustard | 9 | 78 | 100 |
| Phacelia | 7 | 71 | 71 |

second RMSE for mustard, the validation RMSE for both crop types (0.62 Mg DM ha$^{-1}$ for phacelia) is roughly twice higher than the model CVRMSE. Nevertheless, knowing the error induced by the estimation of biomass through vegetation height, these results are consistent with the VI-DMB models performances. For mustard, the model seems to overestimate low biomass value (under 1 Mg DM ha$^{-1}$) but this can be linked to an underestimation of biomass by the height-DMB model. For phacelia, the range of validation data is limited and the high biomass values appear more challenging for the model.

### 3.3. Added-value of the RS models

Comparisons of biomass values distributed over different classes at field level, estimated on the one hand either on farmers-based observations or based on selected RS-models, and on the other hand with the plant sample-based estimations, are presented in Fig. 13. Biomass values estimated by farmers or RS-based models tend to be generally higher than the ones estimated from plant sample-based measurements, considered as the reference method. This is particularly true for the mixed winter cover crops and the full data set of winter cover crops. Results between model and reference method are very good for pure stand mustard, while good for pure stand phacelia. From Table 3, we can conclude that the classifications of mustard biomass level using RS-based models are more accurate than the farmers estimations and reach the same accuracy for phacelia biomass. For mixed stands (and all crop types together), farmers classification is slightly more accurate than RS-based classification.

These results are based on the strong assumption that the four samples collected per field are representative of the whole field. Though the sampling points have been selected so as to integrate the intra-field heterogeneity, this assumption could be questionable. The direct comparison of biomass classes estimated on the one hand by the RS-models and on the other hand by the farmers highlights their convergence; estimated biomass classes are identical for 25 fields over 35 (Fig. 14). This can be explained by the fact that both estimations considered the whole field area and not samples. On the other hand, Fig. 13 shows that farmers and RS-models approaches do not fail in the same way. This would have been probably the case if the sampling were poorly representative of the whole field.

## 4. Discussion

For each of the four winter cover crop categories considered in our study (mustard, phacelia, mixed and full *i.e.* whole types together), an empirical model considering the relationship linking the DMB and a VI has been identified. The methodology assessed a range of different empirical models, concluding that several models were as good as the four described in Fig. 7, as illustrated in Figs. 5 and 6. Also, the model ranking is certainly sensitive to the distribution of each category considered. It could be different, for instance, by reducing the range of biomass of one category by putting aside one crop of the dataset.

Except for CVI, suitable specifically for mustard biomass estimation, a saturation of the VI can be observed for high values of DMB, usually above 2 Mg DM ha$^{-1}$. As stated in the results, CVI is probably not good when the crop reflectance is close to bare soil, showing that it is necessary to ensure there is sufficient canopy covering of soil before using this VI practically, for example by using NDVI first. The overestimation of low biomass value in the validation steps reinforced this assumption. Moreover, the validation steps showed that the models are somehow limited for high biomass value because higher CVI than observed in the model dataset were possible for similar high biomass values. An easy way to handle this practically could be to set the biomass value at the maximum value of the model when CVI is higher to the maximum CVI of the model.

Despite the assessment of the whole panel of 10 and 20 m bands of S2 through VIs, including RE bands, supposed to enhance the biomass estimation, (Delegido et al., 2011), the saturation issues were not completely solved, even if saturation appears at higher biomass levels than those observed for cereals winter cover crops by Hively et al. (2009) and Prabhakara et al. (2015). Studies showed that the use of RE bands does not always improve biophysical parameters retrieval. On one side, Sharma et al. (2015) show that the use of RE, in spite of red band, reduce saturation in corn yield estimation, and Vina et al. (2011) show better results for LAI estimation in maize and soybean using RE VIs (MTCI and CI RE). On the other side, Kross et al. (2015) observed similar performances of RE and other VIs for LAI and biomass estimation of maize and soybean and Clevers et al. (2017) highlighted similar conclusions for the LAI and CCC of potato crops. In our case, RE seems to improve the biomass estimation and reduces saturation issues, at least for phacelia and mixed categories, for which the model selected uses a RE VI.

The second approach tested in this study to tackle the saturation issues by using a different VI for low and high biomass values (Nguy-Robertson et al., 2012) showed that VIs highlighted for biomass values under 2 Mg DM ha$^{-1}$ performed very well, even for the mixed and 'full' categories. For values above 2 Mg DM ha$^{-1}$, the results were significantly worse even though the curves did not show saturation issues. This shows that these high values are still difficult to handle with this second approach. Operationally, this approach would necessitate, firstly a distinction between the two groups of biomass, which could be

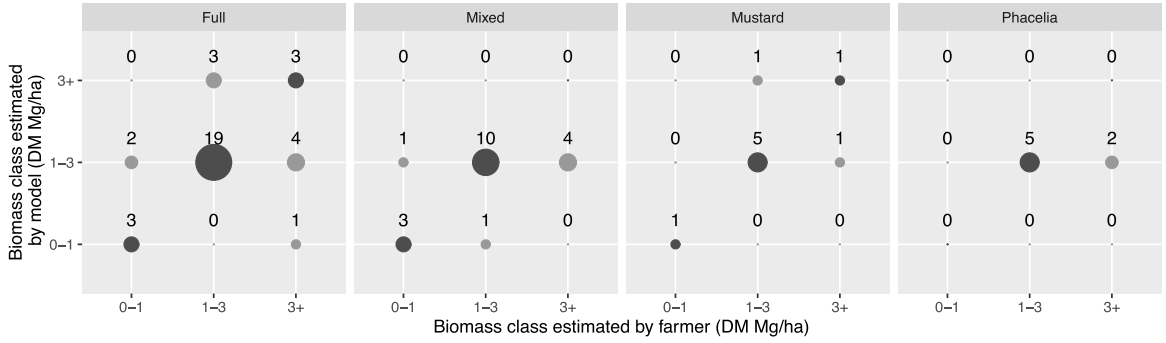


**Fig. 14.** Error matrix of winter cover crops biomass values distributed over different classes and estimated from farmers-based observations versus RS models-based approaches.

done by the model using one VI for the whole range of biomass (approach 1).

This difficulty in handling high biomass values represents a limitation in the context of total nitrogen recommendation, as it limits the possibility to discriminate between medium and high DMB classes (respectively 1–3 and >3 Mg DM $ha^{-1}$). Though particular attention has been paid when selecting sampling points to cover the widest range of DMB situations, these different models have been calibrated/validated mainly using samples from the intermediary biomass class. The model's validity range concerns therefore, mainly one, rather wide (2 Mg DM $ha^{-1}$), DMB class. The relevance of these models in total nitrogen recommendation systems based on DMB classes, is therefore rather limited, but could positively contribute in systems based on continuous values, especially for winter cover crop types with a maximum DMB usually lower than 2.5–3 Mg DM $ha^{-1}$, such as phacelia. This statement is reinforced by the fact that farmers provide qualitative information on the DMB available in their different fields. The farmer has just to specify if the biomass is "low", "medium" or "high". Moving from a qualitative to a quantitative estimation of the biomass level can be complicated, especially for mixed stands that can be very diversified in terms of floristic composition, and subsequently in their structure (height, density, number of vegetation layers, etc.). The increasing occurrence of these mixed stands in the Belgian landscape represents a real challenge in an objective of DMB estimation by satellite RS and more generally in the context of total nitrogen recommendations.

These limitations (saturation issues, limited number of samples) can explain partly why farmers can provide, except for mustard and phacelia, a better estimation of DMB at parcel level than satellite data. Other plausible explanations can be proposed. The reference DMB at parcel level is first of all based on a limited number of samples which, though collected in homogeneous areas within the different parcels, do not necessarily represent the intra-field heterogeneity. Using classes can also induce errors especially for situations at the different defined boundaries classes.

Different ways to go further in this study can be considered. Models were calibrated and validated based on data acquired only for one year. Considering data for several years would allow an increase in the calibration range. In the same way, it would be also interesting to take regular samples during the growing period, in order to better evaluate the relationship linking biomass and VIs. One of the limitations of our study is the cloudy conditions hampering the use of optical satellites such as S2 and leading to the impossibility to use S2 data in 2016 and to a non systematic coincidence between sampling and image acquisition dates in 2017. A possible solution to address this problem could be the use of SAR data like Sentinel-1, for instance through the use of VV, VH or their ratio (Veloso et al., 2017). More sophisticated empirical regression techniques such as ANN (Artificial Neural Network) or decision tree/random forest regression (as suggested by Wang et al., 2016) could also be tested. However these techniques require a lot of observations and a very intensive field campaign would need to be organised.

Furthermore, some crop growth models such as STICS are now also able to simulate growth of some winter cover crops such as mustard or rye-grass (Dorsainvil, 2002). Using these models, possibly combined with satellite data, through assimilation techniques represents another way that could be followed to estimate winter cover crop biomass.

## 5. Conclusion

These findings have to be considered as a first research results in a topic never addressed in literature to our knowledge, *i.e.* assessing the potentialities of S2 satellite data for estimating the DMB of the green manure winter cover crops in intensive cropping systems. The resulting models can assess the biomass level for mustard, phacelia, and mixed cover crops, to be used as an input for nitrogen fertilization recommendation frameworks. Models performed twice better for pure stands cover crops (mustard and phacelia) than for mixed cover and allow classifying the biomass in the three classes required for the nitrogen provisional balance sheet method. A remaining challenge concerns these mixed cover crops to be further investigated possibly by stratifying the mixed cover crops according to similar canopies. The saturation issues were not solved for phacelia and mixed cover crops with high biomass levels. A possible limitation of S2 images is the cloud occurrence, which can be high in the period of interest (mainly autumn) in various Northern European countries.

## Credit author statement

**Dimitri Goffart**: Conceptualization, Methodology, Software, Formal analysis, Investigation, Data curation, Writing – Original Draft, Writing – Review & Editing, Visualization.

**Yannick Curnel**: Conceptualization, Methodology, Investigation, Writing – Review & Editing, Supervision, Funding Acquisition.

**Viviane Planchon**: Conceptualization, Methodology, Resources, Project Administration.

**Jean-Pierre Goffart**: Conceptualization, Methodology, Resources, Writing – Review & Editing, Funding Acquisition, Supervision.

**Pierre Defourny**: Conceptualization, Writing – Review & Editing, Funding Acquisition, Supervision.

## Funding

This work was supported by the SPP Politique scientifique – BELSPO under GrantSR/00/300 – BELCAM.

## Conflicts of interest

None declared.

## Declaration of Competing Interest

The authors report no declarations of interest.

## Acknowledgements

Many thanks to all the farmers who allowed us to take samples in their fields, to the CRA-W crew who contributed to the field work (Amaury Leclef, Gregory Clou, Daniel Deloos and William Philippe) and to Isabelle Piccard from VITO (BELCAM project partner) for the access to the L2A level Sentinel-2 images.

R (R Core Team, 2018) was used for the data processing. Thanks to the whole team and community for developing such a powerful and versatile tool.

## Appendix A. Vegetation indices tested with S2 images for winter cover crop biomass retrieval

**Table A.4**
Vegetation indices tested with S2 images for winter cover crop biomass retrieval.

| Original acronym | Index | Used acronym | (Derived) S2 Formula | Source | Original author |
|---|---|---|---|---|---|
| Chlogreen | Chlorophyll Green index | Chlogreen | $B_{8A}/(B_3+B_5)$ | Radoux et al., 2016 | Datt, 1999 |
| CIGr | Green Chlorophyll Index | CIGr | $B_8/B_3-1$ | Clevers et al., 2017 | Gitelson et al., 2003 |
| CIGr | Green Chlorophyll Index | CIGr2 | $B_{8A}/B_3-1$ | Vina et al., 2011 | Gitelson et al., 2003 |
| CIRe | Red-edge Chlorophyll Index | CIRe | $B_7/B_5-1$ | Clevers et al., 2017 | Gitelson et al., 2003 |
| ClRe | Red-edge Chlorophyll Index | ClRe2 | $B_{8A}/B_5-1$ | Vina et al., 2011 | Gitelson et al., 2003 |
| CRI | Carotenoid Reflectance Index | CRI | $1/B_3+1/B_8$ | Wang et al., 2016 | Gitelson et al., 2002 |
| CVI | Chlorophyll Vegetation Index | CVI | $(B_8/B_3)(B_4/B_3)$ | Clevers et al., 2017 | Vincini et al., 2008 |
| EVI | Enhanced Vegetation Index | EVI | $2.5\frac{(B_8-B_4)}{B_8+6B_4-7.5B_2+1}$ | Wang et al., 2016; Prabhakara et al., 2014 | Liu and Huete, 1995 |
| EVI2 | Enhanced Vegetation Index 2 | EVI2 | $2.5\frac{(B_8-B_4)}{B_8+2.4B_4+1}$ | Sentinel Hub | |
| EVI | Enhanced Vegetation Index | EVI8a | $2.5\frac{B_{8A}-B_4}{B_{8A}+6B_4-7.5B_2+1}$ | Vina et al., 2011 | Huete et al., 1996 |
| GEMI | Global Environment Monitoring Vegetation Index | GEMI | $\frac{2(B_{8A}^2-B_4^2)+1.5B_{8A}+0.5B_4}{B_{8A}+B_4+0.5}$ | Radoux et al., 2016 | Pinty and Verstraete, 1992 |
| GI | Greenness Index | GI | $B_3/B_4$ | Radoux et al., 2016 | le Maire et al., 2004 |
| GNDVI73 | Green Normalized Difference Vegetation Index | GNDVI73 | $(B_7-B_3)/(B_7+B_3)$ | Frampton et al., 2013 | Gitelson et al. (1996) |
| GNDVI | Green-NDVI | GNDVI83 | $(B_8-B_3)/(B_8+B_3)$ | Wang et al., 2016; Prabhakara et al., 2014 | Gitelson et al., 1996 |
| gNDVI | Green normalized difference vegetation index | GNDVI8a3 | $(B_{8A}-B_3)/(B_{8A}+B_3)$ | Radoux et al., 2016 | Gitelson et al., 1996 |
| GR | Green minus Red | GR | $B_3-B_4$ | Prabhakara et al., 2014 | |
| GRVI1 | | GRVI1 | $(B_4-B_3)/(B_4+B_3)$ | Sentinel Hub | |
| IRECI | Inverted Red-Edge Chlorophyll Index | IRECI | $(B_7-B_4)/(B_5/B_6)$ | Frampton et al., 2013 | Frampton et al., 2013 |
| LAI.SAVI | | LAI_SAVI | $-\log(0.371+1.5(B_8-B_4)/(B_8+B_4+0.5))/2.4$ | Sentinel Hub | |
| MCARI | Modified Chlorophyl Absorption in Reflectance Index | MCARI | $((B_5-B_4)-0.2(B_5-B_3))(B_5-B_4)$ | Frampton et al., 2013 | Daughtry et al. (2000) |
| MSAVI2 | | MSAVI2 | $(B_8+1)-0.5\sqrt{(2B_8-1)^2+8B_4}$ | Sentinel Hub | |
| MSI | Moisture stress index | MSI | $B_{11}/B_{8A}$ | Radoux et al., 2016 | Rock, B.N. et al., 1985 |
| MSR | Modified Simple Ratio Index | MSR | $(B_8/B_4-1)/\sqrt{B_8/B_4+1}$ | Wang et al., 2016 | Chen, 1996 |
| MTCI | MERIS Terrestrial Chlorophyll Index | MTCI | $(B_6-B_5)/(B_5-B_4)$ | Frampton et al., 2013 | Dash and Curran (2004) |
| MTCI2 | MERIS Terrestrial Chlorophyll Index | MTCI8a | $(B_{8A}-B_5)/(B_5-B_4)$ | Vina et al., 2011 | Dash and Curran, 2004 |
| MTVI2 | Modified Triangular Vegetation Index 2 | MTVI2 | $1.5\frac{1.2(B_8-B_3)-2.5(B_4-B_3)}{\sqrt{2B_8+12-6B_8+5\sqrt{B_4}}-0.5}$ | Wang et al., 2016 | Haboudane et al., 2004 |
| NAOC | Normalized Area Over the reflectance Curve | NAOC | $1-(40(B_4+B_5)/2+35(B_5+B_6)/2+43(B_6+B_7)/2)/(118B_7)$ | Delegido et al., 2011 | |
| NDReSw | Normalized Difference of Red-edge and SWIR2 | NDReSw | $(B_6-B_{12})/(B_6+B_{12})$ | Radoux et al., 2016 | |
| NDTI | Normalized Difference Tillage Index | NDTI | $(B_{11}-B_{12})/(B_{11}+B_{12})$ | Radoux et al., 2016 | Van Deventer et al., 1997 |
| NDVI.Gr | | NDVI_Gr | $B_3(B_8-B_4)/(B_8+B_4)$ | Sentinel Hub | |
| NDI45 | Normalized Difference Vegetation Index optimum for S2 | NDVI5 | $(B_5-B_4)/(B_5+B_4)$ | Frampton et al., 2013; Delegido et al., 2011 | Delegido et al. (2011b) |
| NDI | Normalized Difference Index | NDVI6 | $(B_6-B_4)/(B_6+B_4)$ | Prabhakara et al., 2014; Delegido et al., 2011 | Gitelson and Merzlyak, 1994 |
| NDVI | Normalized Difference Vegetation Index | NDVI7 | $(B_7-B_4)/(B_7+B_4)$ | Frampton et al., 2013; Sharma et al., 2015; Delegido et al., 2011 | Rouse et al. (1973) |
| NDVI | Normalized Difference Vegetation Index | NDVI8 | $(B_8-B_4)/(B_8+B_4)$ | Wang et al., 2016; Prabhakara et al., 2014; Delegido et al., 2011 | Rouse et al., 1974 |
| NDVI | Normalized Difference Vegetation Index | NDVI8a | $(B_{8A}-B_4)/(B_{8A}+B_4)$ | Vina et al., 2011; Radoux et al., 2016; Delegido et al., 2011 | Rouse et al., 1974 |
| NDWI1 | Normalized Difference Water Index 1 | NDWI1 | $(B_{8A}-B_{11})/(B_{8A}+B_{11})$ | Radoux et al., 2016 | Gao, 1996 |
| NDWI2 | Normalized Difference Water Index 2 | NDWI2 | $(B_3-B_{8A})/(B_3+B_{8A})$ | Radoux et al., 2016 | Mcfeeters, 1996 |
| NGRDI | Normalized Green Red Difference Index | NGRDI | $(B_3-B_4)/(B_3+B_4)$ | Prabhakara et al., 2014; Wang et al., 2016 | Tucker, 1979 |
| NHI | Normalized Humidity Index | NHI | $(B_{11}-B_3)/(B_{11}+B_3)$ | Radoux et al., 2016 | Lacaux, 2007 |
| NLI | Nonlinear Vegetation Index | NLI | $(B_8^2-B_4)/(B_8^2+B_4)$ | Wang et al., 2016 | Goel and Qin, 1994 |
| OSAVI | Optimized Soil-Adjusted Vegetation Index | OSAVI | $1.16(B_8-B_4)/(B_8+B_4+1.6)$ | Wang et al., 2016 | Rondeaux et al., 1996 |
| PSRI | Plant Senescence Reflectance Index | PSRI | $(B_4-B_2)/B_8$ | Wang et al., 2016 | Merzlyak et al., 1999 |
| RDVI | Re-normalized Difference Vegetation Index | RDVI | $(B_8-B_4)/\sqrt{B_8+B_4}$ | Wang et al., 2016 | Wang et al., 1998 |
| RedSWIR1 | Bands difference | RedSWIR1 | $B_4-B_{11}$ | Radoux et al., 2016 | Jacques et al., 2014 |
| NDI | Normalized Difference Index | RENDVI65 | $(B_6-B_5)/(B_6+B_5)$ | Delegido et al., 2011 | |
| RENDVI | Red-Edge Normalized Difference Vegetation Index | RENDVI75 | $(B_7-B_5)/(B_7+B_5)$ | Sharma et al., 2015; Delegido et al., 2011 | |
| RENDVI | Red-Edge Normalized Difference Vegetation Index | RENDVI76 | $(B_7-B_6)/(B_7+B_6)$ | Sharma et al., 2015; Delegido et al., 2011 | |
| NDI | Normalized Difference Index | RENDVI85 | $(B_8-B_5)/(B_8+B_5)$ | Delegido et al., 2011 | |

(*continued on next page*)

**Table A.4** (*continued*)

| Original acronym | Index | Used acronym | (Derived) S2 Formula | Source | Original author |
|---|---|---|---|---|---|
| NDI | Normalized Difference Index | RENDVI86 | $(B_8 - B_6)/(B_8 + B_6)$ | Delegido et al., 2011 | |
| NDVIre | Red-edge normalized difference vegetation index | RENDVI8a5 | $(B_{8A} - B_5)/(B_{8A} + B_5)$ | Radoux et al., 2016; Delegido et al., 2011 | Gitelson et al., 1996 |
| NDI | Normalized Difference Index | RENDVI8a6 | $(B_{8A} - B_6)/(B_{8A} + B_6)$ | Delegido et al., 2011 | |
| RePA | Red-edge peak area | RePA | $B_4 + B_5 + B_6 + B_7 + B_{8A}$ | Radoux et al., 2016 | |
| RTVIcore | Red-edge Triangular Vegetation Index | RTVIcore | $100(B_{8A} - B_5) - 10(B_{8A} - B_3)$ | Radoux et al., 2016 | Chen et al., 2010 |
| S2REP | Sentinel 2 red-edge position | S2REP | $705 + 35((((B_7 + B_4)/2) - B_5)/(B_6 - B_5))$ | Frampton et al., 2013 | Frampton et al., 2013 |
| SAVI | Soil-Adjusted Vegetation Index | SAVI | $1.5(B_8 - B_4)/(B_8 + B_4 + 0.5)$ | Wang et al., 2016; Prabhakara et al., 2014 | Huete, 1998 |
| SAVI | Soil Adjusted Vegetation Index | SAVI8a | $0.5(B_{8A} - B_4)/(B_{8A} + B_4 + 0.5)$ | Radoux et al., 2016 | Huete, 1988 |
| SIPI | Structure Insensitive Pigment Index | SIPI | $(B_8 - B_2)/(B_8 + B_2)$ | Wang et al., 2016 | Penuelas et.al, 1995 |
| SRBlRe1 | Simple Blue and Red-edge 1 Ratio | SR25 | $B_2/B_5$ | Radoux et al., 2016 | le Maire et al., 2004 |
| SRBlRe2 | Simple Blue and Red-edge 2 Ratio | SR26 | $B_2/B_6$ | Radoux et al., 2016 | Lichtenthaler et al., 1996 |
| SRBlRe3 | Simple Blue and Red-edge 3 Ratio | SR27 | $B_2/B_7$ | Radoux et al., 2016 | Derived from le Maire et al., 2004, Lichtenthaler et al., 1996 |
| PSSRa | Pigment Specific Simple Ratio | SR74 | $B_7/B_4$ | Frampton et al., 2013 | Blackburn (1998) |
| SR | Simple Ratio | SR84 | $B_8/B_4$ | Prabhakara et al., 2014; Wang et al., 2016 | Tucker and Sellers, 1986 |
| SRNIRBl | Simple ratio NIR narrow and Blue | SR8a2 | $B_{8A}/B_2$ | Radoux et al., 2016 | Blackburn, 1998 |
| SRNIRGr | Simple ratio NIR narrow and Green | SR8a3 | $B_{8A}/B_3$ | Radoux et al., 2016 | le Maire et al., 2004 |
| SR | Simple Ratio | SR8a4 | $B_{8A}/B_4$ | Vina et al., 2011; Radoux et al., 2016 | Jordan, 1969 |
| SRNIRRe1 | Simple NIR and Red-edge 1 Ratio | SR8a5 | $B_{8A}/B_5$ | Radoux et al., 2016 | Datt, 1999 |
| SRNIRRe2 | Simple NIR and Red-edge 2 Ratio | SR8a6 | $B_{8A}/B_6$ | Radoux et al., 2016 | Derived from Datt, 1999 |
| SRNIRRe3 | Simple NIR and Red-edge 3 Ratio | SR8a7 | $B_{8A}/B_7$ | Radoux et al., 2016 | Derived from Datt, 1999 |
| STI | Soil Tillage Index | STI | $B_{11}/B_{12}$ | Radoux et al., 2016 | Van Deventer et al., 1997 |
| TCARI/ OSAVI | Transformed Chloropyll Adjusted Reflectance Indice/Optimized Soil Adjusted Vegetation Index | TCARI_ OSAVI | $3\frac{(B_5 - B_4) - 0.2(B_5 - B_3)(B_5/B_4)}{(1 + 0.16)(B_7 - B_4)/(B_7 + B_4 + 0.16)}$ | Clevers et al., 2017 | Haboudane et al., 2002 |
| TVI | Transformational Vegetation Index | TNDVI | $\sqrt{(B_8 - B_4)/(B_8 + B_4) + 0.5}$ | Wang et al., 2016 | Broge and Leblanc, 2000 |
| TVI | Triangular Vegetation Index | TVI | $0.5(120(B_8 - B_3) - 200(B_4 - B_3))$ | Prabhakara et al., 2014 | Broge and Leblanc, 2000 |
| VARI | Visible Atmospherically Resistant Index | VARI | $(B_3 - B_4)/(B_3 + B_4 - B_2)$ | Prabhakara et al., 2014 | Gitelson et al., 2002 |

## References


Besnard, A., Le Gall, A., 2000. Les cultures fourrageres intermediaires: pieges à nitrates et fourrages d'appoint? Fourrages 163, 293–306.

Clevers, J., Kooistra, L., van den Brande, M., 2017. Using Sentinel-2 data for retrieving LAI and leaf and canopy chlorophyll content of a potato crop. Remote Sens. 9, 405. https://doi.org/10.3390/rs9050405. http://www.mdpi.com/2072-4292/9/5/405.

Cugnon, T., Toussaint, B., Balon, J., Blondiau, L.M., Collin, C., Heens, B., Coutisse, C., Lizin, P., Lambert, R., 2013. Etablissement du conseil de fumure azotee en cultures, preconise par l'ASBL REQUASUD.

Dash, J., Curran, P.J., 2004. The MERIS terrestrial chlorophyll index. Int. J. Remote Sens. 25, 5403–5413. https://doi.org/10.1080/0143116042000274015.

Delegido, J., Verrelst, J., Alonso, L., Moreno, J., 2011. Evaluation of Sentinel-2 red-edge bands for empirical estimation of green LAI and chlorophyll content. Sensors 11, 7063–7081. https://www.mdpi.com/1424-8220/11/7/7063.

Destain, J.P., Reuter, V., Goffart, J.P., 2010. Les cultures intermediaires pieges a nitrate (CIPAN) et engrais verts: protection de l'environnement et interet agronomique. Biotechnol. Agron. Soc. Environ. 6.

Dorsainvil, F., 2002. Evaluation par modelisation de l'impact environnemental des modes de conduite des cultures intermediaires sur les bilans d'eau et d'azote dans les systemes de culture. INAPG. Ph.D. Thesis.

ESA, 2012. Sentinel-2, ESA's Optical High-Resolution Mission for GMES Operational Services. ESA. Technical Report.

EUROSTAT, 2018. Farm Structure Survey 2016 [News Release]. https://ec.europa.eu/eurostat/documents/2995521/9028470/5-28062018-AP-EN.pdf.

Fang, S., Tang, W., Peng, Y., Gong, Y., Dai, C., Chai, R., Liu, K., 2016. Remote estimation of vegetation fraction and flower fraction in oilseed rape with unmanned aerial vehicle data. Remote Sens. 8, 416. https://doi.org/10.3390/rs8050416. http://www.mdpi.com/2072-4292/8/5/416.

Frampton, W.J., Dash, J., Watmough, G., Milton, E.J., 2013. Evaluating the capabilities of Sentinel-2 for quantitative estimation of biophysical variables in vegetation. ISPRS J. Photogram. Remote Sens. 82, 83–92. https://doi.org/10.1016/j.isprsjprs.2013.04.007. http://www.sciencedirect.com/science/article/pii/S092427161300107X.

Hively, W.D., Lang, M., McCarty, G.W., Keppler, J., Sadeghi, A., McConnell, L.L., 2009. Using satellite remote sensing to estimate winter cover crop nutrient uptake efficiency. J. Soil Water Conserv. 64, 303–313. https://doi.org/10.2489/jswc.64.5.303. http://www.jswconline.org/content/64/5/303.

Hunt, E.R., Hively, W.D., McCarty, G.W., Daughtry, C.S.T., Forrestal, P.J., Kratochvil, R. J., Carr, J.L., Allen, N.F., Fox-Rabinovitz, J.R., Miller, C.D., 2013. NIR-green-blue high-resolution digital images for assessment of winter cover crop biomass. GISci. Remote Sens. https://doi.org/10.2747/1548-1603.48.1.86?needAccess=true.

Jaramaz, D., Perovic, V., Belanovic, S., 2013. The ESA Sentinel-2 Mission Vegetation Variables for Remote Sensing of Plant Monitoring.

Justes, E., Beaudoin, N., Bertuzzi, P., Charles, R., Constantin, J., Durr, C., Hermon, C., Joannon, A., Le Bas, C., Mary, B., Mignolet, C., Montfort, F., Ruiz, L., Sarthou, J.P., Souchere, V., Tournebize, J., 2012. Reduire les fuites de nitrate au moyen de cultures intermediaires: consequences sur les bilans d'eau et d'azote, autres services ecosystemiques. Report. http://oatao.univ-toulouse.fr/16383/.

Kalaitzidis, C., Heinzel, V., Zianis, D., 2009. A Review of Multispectral Vegetation Indices for Biomass Estimation.

Kross, A., McNairn, H., Lapen, D., Sunohara, M., Champagne, C., 2015. Assessment of RapidEye vegetation indices for estimation of leaf area index and biomass in corn and soybean crops. Int. J. Appl. Earth Observ. Geoinf. 34, 235–248. https://doi.org/10.1016/j.jag.2014.08.002. http://www.sciencedirect.com/science/article/pii/S0303243414001664.

Kuo, S., Sainju, U.M., Jellum, E.J., 1996. Winter cover cropping influence on nitrogen mineralization, presidedress soil nitrate test, and corn yields. Biol. Fertil. Soils 22, 310–317. https://doi.org/10.1007/BF00334575.

Labreuche, J., 2009. Cultures intermediaires: La destruction du couvert, une etape cruciale. Perspect. Agric. 36–41.

Nguy-Robertson, A., Gitelson, A., Peng, Y., Viña, A., Arkebauer, T., Rundquist, D., 2012. Green leaf area index estimation in maize and soybean: combining vegetation indices to achieve maximal sensitivity. Agron. J. 104, 1336–1347. https://doi.org/10.2134/agronj2012.0065. https://dl.sciencesocieties.org/publications/aj/abstracts/104/5/1336.

Prabhakara, K., Hively, W.D., McCarty, G.W., 2015. Evaluating the relationship between biomass, percent groundcover and remote sensing indices across six winter cover crop fields in Maryland, United States. Int. J. Appl. Earth Observ. Geoinf. 39, 88–102. https://doi.org/10.1016/j.jag.2015.03.002. http://www.sciencedirect.com/science/article/pii/S0303243415000525.

R Core Team, 2018. R: A Language and Environment for Statistical Computing. R Foundation for Statistical Computing, Vienna, Austria. https://www.R-project.org/.

Radoux, J., Chome, G., Jacques, D.C., Waldner, F., Bellemans, N., Matton, N., Lamarche, C., d'Andrimont, R., Defourny, P., 2016. Sentinel-2's potential for sub-pixel landscape feature detection. Remote Sens. 8 https://doi.org/10.3390/rs8060488. http://www.mdpi.com/2072-4292/8/6/488.

Rock, B., Vogelmann, J., Williams, D.L., 1985. Field and airborne spectral characterization of suspected damage in red spruce (picea rubens) from Vermont. International Symposium – Machine Processing of Remotely Sensed Data.

Sharma, L.K., Bu, H., Denton, A.M., Franzen, D.W., 2015. Active-optical sensors using red NDVI compared to red edge ndvi for prediction of corn grain yield in North Dakota, U.S.A. Sensors.

SPW, 2017. Notice explicative de la declaration de superficie et demande d'aides 2017, 2eme volet: Aperçu des legislations – Conditionnalite – Controles.
Sterckx, S., Knaeps, E., Adriaensen, S., Reusen, I., De Keukelaere, L., Hunter, P., Giardino, C., Odermatt, D., 2015. OPERA: An Atmospheric Correction For Land And Water.
Sulik, J.J., Long, D.S., 2015. Spectral indices for yellow canola flowers. Int. J. Remote Sens. 36, 2751–2765. https://doi.org/10.1080/01431161.2015.1047994.
Takeno, Kiyotoshi, 2016. Stress-induced flowering: the third category of flowering response. J. Exp. Bot. 67 https://doi.org/10.1093/jxb/erw272.
Veloso, A., Mermoz, S., Bouvet, A., Le Toan, T., Planells, M., Dejoux, J.F., Ceschia, E., 2017. Understanding the temporal behavior of crops using Sentinel-1 and Sentinel-2-like data for agricultural applications. Remote Sens. Environ. 199, 415–426. https://doi.org/10.1016/j.rse.2017.07.015. https://linkinghub.elsevier.com/retrieve/pii/S0034425717303309.
Vina, A., Gitelson, A.A., Nguy-Robertson, A.L., Peng, Y., 2011. Comparison of different vegetation indices for the remote assessment of green leaf area index of crops. Remote Sens. Environ. 115, 3468–3478. https://doi.org/10.1016/j.rse.2011.08.010. http://linkinghub.elsevier.com/retrieve/pii/S0034425711002926.
Vincini, M., Frazzi, E., D'Alessio, P., 2008. A broad-band leaf chlorophyll vegetation index at the canopy scale. Precis. Agric. 9, 303–319. https://doi.org/10.1007/s11119-008-9075-z.
Wang, L., Zhou, X., Zhu, X., Dong, Z., Guo, W., 2016. Estimation of biomass in wheat using random forest regression algorithm and remote sensing data. Crop J. 4, 212–219. https://doi.org/10.1016/j.cj.2016.01.008. http://www.sciencedirect.com/science/article/pii/S2214514116300162.
Weiss, M., Baret, F., 2016. S2ToolBox Level 2 Products: LAI, FAPAR, FCOVER, Version 1.1.
Xue, J., Su, B., 2017. Significant Remote Sensing Vegetation Indices: A Review of Developments and Applications. https://doi.org/10.1155/2017/1353691. , ISSN: 1687-725X Library Catalog: www.hindawi.com Pages: e1353691 Publisher: Hindawi Volume: 2017. https://www.hindawi.com/journals/js/2017/1353691/.
Yuan, M., Burjel, J.C., Isermann, J., Goeser, N.J., Pittelkow, C.M., 2019. Unmanned aerial vehicle-based assessment of cover crop biomass and nitrogen uptake variability. J. Soil Water Conserv. 74, 350–359. https://doi.org/10.2489/jswc.74.4.350. http://www.jswconline.org/content/74/4/350.